Unified Biquaternion Theory (Consolidation) — CORE Manuscript

UBT Team

August 11, 2025

Contents

A Biquaternion Gravity **2**
A.1 Introduction . . . 2
A.2 Core Equations . . . 2
A.3 analysis Summary . . . 3
A.4 Summary . . . 3

A Overview **3**

B Biquaternion Formulation of Electromagnetism **3**

C Maxwell's Equations in Curved Spacetime **4**

D Original analysis Notes **4**

E Wave Solutions **4**

F Field Invariants and Duality **4**

G Links to Other Appendices **4**

A Appendix D: Quantum Electrodynamics (QED) in the Unified Biquaternion Theory **5**

B UBT Extension of QED **8**

C Appendix E: Standard Model Coupling and QCD Embedding in UBT **10**
C.1 Overview . . . 10
C.2 Gauge bundle and connections . . . 10
C.3 UBT → SM dictionary . . . 10
C.4 Gauge-invariant Lagrangian . . . 10
C.5 Running couplings and matching . . . 11
C.6 Topological interpretation of QCD in UBT . . . 11
C.7 Matching conditions and open tasks . . . 11
C.8 Consistency with dark matter appendix . . . 11

A Appendix P: Bibliography **14**

B Policy on the Fine-Structure Constant **14**

CORE Scope and Claims

This CORE manuscript presents a biquaternion formulation that recovers the Einstein–Maxwell–Dirac system under a standard variational action and demonstrates the correct limits (Minkowski and weak-field). **We do not claim an ab-initio derivation of the fine-structure constant** α; in the CORE track $\alpha(\mu)$ is treated as an empirical input consistent with QED running. Any links between the auxiliary phase coordinate ψ and consciousness are considered *interpretive and speculative* and are not part of the CORE results. Quantitative, testable predictions are stated with their assumptions and orders of magnitude.

A Biquaternion Gravity

This appendix presents the gravitational sector of the Unified Biquaternion Theory (UBT). It combines the core theoretical framework from the original Biquaternion Gravity appendix with the detailed analysis from the Quantum Gravity solution files, reformulated for clarity and coherence.

A.1 Introduction

The gravitational field in UBT emerges naturally from the covariant formulation of the biquaternionic tensor-spinor field equations. The metric tensor is propose from the real part of the scalar product in the biquaternion space, ensuring compatibility with the principles of General Relativity while extending them to the complexified algebraic structure.

In this formulation, spacetime is represented by a projection from a higher-dimensional complex manifold, and curvature is encoded in the covariant derivatives of the biquaternion field $\Theta(q, \tau)$. The gravitational interaction is therefore not an independent postulate, but a manifestation of the underlying field geometry.

A.2 Core Equations

The line element is expressed as:

$$ds^2 = g_{\mu\nu}\, dx^\mu dx^\nu, \tag{1}$$

where the metric tensor $g_{\mu\nu}$ is obtained from the biquaternion field via:

$$g_{\mu\nu} = \Re\left[\frac{\partial_\mu \Theta \cdot \partial_\nu \Theta^\dagger}{\mathcal{N}}\right], \tag{2}$$

with $\mathcal{N}$ a normalisation factor ensuring the correct signature.

The Einstein tensor in this framework takes the standard form:

$$G_{\mu\nu} = R_{\mu\nu} - \frac{1}{2} g_{\mu\nu} R, \tag{3}$$

but with curvature tensors $R_{\mu\nu}$ and R propose from the biquaternionic connection coefficients $\Gamma^\rho_{\mu\nu}$ obtained from the extended algebra.

The gravitational field equations couple $G_{\mu\nu}$ to the stress-energy tensor $T_{\mu\nu}$ constructed from the biquaternion field invariants:

$$G_{\mu\nu} = 8\pi G\, T_{\mu\nu}[\Theta]. \tag{4}$$

A.3 analysis Summary

The original analysis proceeds by first defining the biquaternionic connection compatible with the metric propose from $\Theta(q, \tau)$. The connection coefficients are computed as:

$$\Gamma^{\rho}_{\mu\nu} = \frac{1}{2} g^{\rho\sigma} \left(\partial_\mu g_{\nu\sigma} + \partial_\nu g_{\mu\sigma} - \partial_\sigma g_{\mu\nu} \right), \tag{5}$$

where $g_{\mu\nu}$ is substituted from the field definition above.

The curvature tensor $R^{\rho}{}_{\sigma\mu\nu}$ is then obtained from:

$$R^{\rho}{}_{\sigma\mu\nu} = \partial_\mu \Gamma^{\rho}_{\nu\sigma} - \partial_\nu \Gamma^{\rho}_{\mu\sigma} + \Gamma^{\rho}_{\mu\lambda} \Gamma^{\lambda}_{\nu\sigma} - \Gamma^{\rho}_{\nu\lambda} \Gamma^{\lambda}_{\mu\sigma}. \tag{6}$$

Contracting appropriately yields $R_{\mu\nu}$ and the scalar curvature R.

In the quantum gravity extension, fluctuations of the field Θ are quantised, leading to corrections to the classical curvature in the form of effective stress-energy terms arising from vacuum polarisation effects. The semiclassical approximation shows that these corrections become significant near the Planck scale, modifying the black hole horizon structure and potentially allowing for stable micro-horizon configurations.

A.4 Summary

Biquaternion Gravity provides a natural embedding of General Relativity into a complexified algebraic framework, unifying gravity with other interactions at the geometric level. The connection to Quantum Gravity arises from treating Θ as a quantum field, where gravitational effects emerge from its covariant structure. This approach suggest possible deviations from classical GR at very small scales, while reducing to Einstein's equations in the macroscopic limit.

CElectromagnetism in the Unified Biquaternion Framework

A Overview

This appendix consolidates the original analysis, solutions, and conceptual notes on electromagnetism within the Unified Biquaternion Theory (UBT). The aim is to present a coherent, non-duplicative treatment, while preserving the original reasoning paths that led to the key results. Links to related appendices on gravitational coupling, α-phase effects, and p-adic extensions are provided where relevant.

B Biquaternion Formulation of Electromagnetism

We start from the covariant field equation for the electromagnetic potential A_μ embedded into the biquaternion algebra $\mathbb{B}$. This allows the electric and magnetic fields to be represented as bivector components of a unified field tensor $\mathcal{F}$,

$$\mathcal{F} = \nabla \wedge A \quad \in \quad \mathbb{B} \otimes \Lambda^2. \tag{7}$$

In explicit biquaternion form:

$$\mathcal{F} = (\mathbf{E} + i\,\mathbf{B}) \cdot \boldsymbol{\sigma}, \tag{8}$$

where $\boldsymbol{\sigma}$ are the Pauli-like basis elements in $\mathbb{B}$ and i is the scalar imaginary unit commuting with the quaternion units.

C Maxwell's Equations in Curved Spacetime

Using the covariant derivative ∇_μ compatible with the UBT metric $g_{\mu\nu}$ propose in Appendix B (Gravitation), Maxwell's equations generalize to:

$$\nabla_\mu \mathcal{F}^{\mu\nu} = \mu_0 J^\nu, \tag{9}$$

$$\nabla_{[\alpha}\mathcal{F}_{\beta\gamma]} = 0. \tag{10}$$

This retains gauge invariance and introduces curvature coupling terms, which in the biquaternion formalism appear as commutator terms $[\Gamma, \mathcal{F}]$ in the connection representation.

D Original analysis Notes

In the early stages of this work, the electromagnetic sector was explored via analogy with the Dirac equation in $\mathbb{B}$. The key insight was that the EM field could be treated as the curvature of a $U(1)$ connection embedded in the right-multiplication sector of $\mathbb{B}$, while the left-multiplication sector described spinorial matter. This decomposition naturally explains charge conjugation symmetry and provides a pathway for coupling to the α-phase field (see Appendix F).

It was also noted that the Fokker–Planck-type diffusion of the ψ-phase in complex time $\tau = t + i\psi$ could modulate the effective permittivity and permeability of the vacuum. This idea connects to the p-adic hierarchical scaling of field strengths (Appendix G).

E Wave Solutions

From the biquaternion Maxwell equations in flat spacetime, one recovers the familiar wave equation:

$$\Box A_\mu = 0, \tag{11}$$

for free fields. In the curved UBT metric, the wave operator becomes the Laplace–Beltrami operator $\Box_g$, leading to redshift and lensing of electromagnetic waves.

Original solution work (see historical "solutions" notes) examined toroidal standing wave configurations, relevant for the Theta Resonator experimental proposal. Such solutions are characterized by localized energy densities and quantized circulation numbers n, potentially linked to the α-quantization of phase space.

F Field Invariants and Duality

Two Lorentz- and gauge-invariant scalars can be formed:

$$\mathcal{I}_1 = \frac{1}{2}\mathcal{F}_{\mu\nu}\mathcal{F}^{\mu\nu} = |\mathbf{B}|^2 - |\mathbf{E}|^2, \tag{12}$$

$$\mathcal{I}_2 = \frac{1}{2}\mathcal{F}_{\mu\nu}\tilde{\mathcal{F}}^{\mu\nu} = 2\,\mathbf{E}\cdot\mathbf{B}. \tag{13}$$

In $\mathbb{B}$ representation, duality rotations correspond to multiplication by $e^{i\theta}$ in the scalar imaginary sector, providing a natural geometric interpretation.

G Links to Other Appendices

- **Appendix B**: Gravitational coupling and metric analysis.
- **Appendix F**: α-phase modulation of EM fields.

- **Appendix G**: p-adic scaling and hierarchical structure of field amplitudes.
- **Appendix H**: Toroidal resonator applications and standing wave quantization.

This appendix should be read alongside these sections to obtain a complete picture of electromagnetism in the UBT framework.

A Appendix D: Quantum Electrodynamics (QED) in the Unified Biquaternion Theory

1. Historical Overview and Core Principles

Quantum Electrodynamics (QED) is the relativistic quantum field theory of the electromagnetic interaction between charged fermions and photons. Built on local $U(1)$ gauge invariance and Lorentz symmetry, QED achieves the most precise agreement between theory and experiment in modern physics (e.g., electron $g-2$, Lamb shift). QED emerged from combining Maxwell's classical electrodynamics with the quantum mechanics of spin-$\frac{1}{2}$ particles (Dirac), and the renormalization program (Feynman, Schwinger, Tomonaga, Dyson).

2. Classical Electrodynamics Recap

The electromagnetic potential A_μ defines the field strength

$$F_{\mu\nu} = \partial_\mu A_\nu - \partial_\nu A_\mu, \tag{14}$$

which satisfies Maxwell's equations (in units with $c = \hbar = 1$ and $\mu_0 = 1$ for simplicity)

$$\partial^\mu F_{\mu\nu} = J_\nu, \qquad \partial_{[\alpha} F_{\beta\gamma]} = 0. \tag{15}$$

The symmetric energy-momentum tensor reads

$$T^{(\mathrm{EM})}_{\mu\nu} = F_{\mu\lambda} F_\nu{}^\lambda - \frac{1}{4}\eta_{\mu\nu} F_{\lambda\sigma} F^{\lambda\sigma}. \tag{16}$$

3. From Classical to Quantum Field Theory

Quantization promotes fields to operators and uses either canonical commutation relations or the path-integral formalism. The free Dirac field obeys

$$(i\gamma^\mu \partial_\mu - m)\psi = 0, \tag{17}$$

with $\{\gamma^\mu, \gamma^\nu\} = 2\eta^{\mu\nu}$.

4. QED Lagrangian and Gauge Symmetry

Local $U(1)$ invariance is implemented by the gauge-covariant derivative

$$D_\mu = \partial_\mu + ieA_\mu, \tag{18}$$

under which $\psi \to e^{ie\alpha(x)}\psi$ and $A_\mu \to A_\mu - \partial_\mu \alpha / e$. The QED Lagrangian density is

$$\mathcal{L}_{\mathrm{QED}} = \bar{\psi}(i\gamma^\mu D_\mu - m)\psi - \frac{1}{4} F_{\mu\nu} F^{\mu\nu}. \tag{19}$$

Euler–Lagrange equations yield the interacting Dirac equation $(i\gamma^\mu D_\mu - m)\psi = 0$ and Maxwell's equations $\partial_\mu F^{\mu\nu} = e\bar{\psi}\gamma^\nu \psi$.

5. Quantization of the Electromagnetic Field

Gauge fixing (e.g., Lorenz gauge $\partial_\mu A^\mu = 0$) leads to the photon propagator. In Faddeev–Popov quantization, the gauge-fixed action includes a term $-\frac{1}{2\xi}(\partial_\mu A^\mu)^2$. Only two transverse photon polarizations are physical.

6. Interaction Terms and Feynman Rules

The interaction Lagrangian

$$\mathcal{L}_{\text{int}} = -e\bar{\psi}\gamma^\mu\psi A_\mu \tag{20}$$

generates the fermion–photon vertex with factor $-ie\gamma^\mu$. The free propagators are $S_F(p) = i(\not{p} - m + i\epsilon)^{-1}$ for fermions and $D_F^{\mu\nu}(k) = \frac{-i}{k^2+i\epsilon}\Big(\eta^{\mu\nu} - (1-\xi)\frac{k^\mu k^\nu}{k^2}\Big)$ for photons (in covariant gauges).

7. Scattering Processes and Cross-Sections

Tree-level amplitudes describe processes such as Compton scattering, Bhabha and Møller scattering, and pair production. Cross-sections follow from $\mathrm{d}\sigma \propto |\mathcal{M}|^2$ with appropriate spin sums/averages and phase space factors.

8. Renormalization in QED

QED is perturbatively renormalizable. Bare parameters (m_0, e_0) and fields $(\psi_0, A_{0\mu})$ are related to renormalized ones via Z-factors:

$$\psi_0 = \sqrt{Z_2}\,\psi, \qquad A_{0\mu} = \sqrt{Z_3}\,A_\mu, \qquad e_0 = Z_e\,e. \tag{21}$$

Ward identities imply $Z_1 = Z_2$ (with Z_1 the vertex renormalization), ensuring charge renormalization consistency.

9. Experimental Verifications of QED

Precision tests include:

- Electron anomalous magnetic moment a_e,
- Lamb shift in hydrogen,
- High-energy scattering (LEP, SLAC) confirming QED couplings.

QED matches experimental data at the level of parts per trillion for some observables.

---

10. UBT Extension of QED

The Unified Biquaternion Theory (UBT) embeds QED as its $U(1)$ sector while extending spacetime to a complex-time manifold and promoting fields to biquaternion-valued objects with additional degrees of freedom. In the limit of constant phase ψ (defined below), the UBT predictions reduce to standard QED.

Complex Time. Define

$$\tau = t + i\psi, \tag{22}$$

where t is the physical time and ψ is the intrinsic phase coordinate associated with the consciousness sector. Derivatives generalize as $\partial_\tau = \partial_t - i\partial_\psi$.

Biquaternionic Field Representation. The master field $\Theta(q,\tau)$ carries spinor/tensor structure in the algebra $\mathbb{B}$ of biquaternions. The electromagnetic potential A_μ appears as a projection of the Θ-connection onto the $U(1)$ subalgebra:

$$A_\mu(x) = \Pi_{U(1)}\big[\mathcal{A}_\mu(\Theta; x, \tau)\big]\Big|_{\psi=\text{const}}. \tag{23}$$

Extended Gauge Transformations. Local $U(1)$ is generalized to phase transformations depending on ψ:

$$\Theta \to e^{iq\alpha(x,\tau)}\Theta, \qquad A_\mu \to A_\mu - \frac{1}{q}\,\partial_\mu\alpha(x,\tau), \tag{24}$$

with the additional relation

$$A_\psi \to A_\psi - \frac{1}{q}\,\partial_\psi\alpha(x,\tau), \tag{25}$$

where A_ψ is the gauge connection along the ψ-direction.

UBT-QED Action. The minimal UBT extension of QED with complex time reads

$$\begin{aligned}\mathcal{L}_{\text{UBT-QED}} = {}& \bar\Psi(i\gamma^\mu D_\mu - m)\Psi - \frac{1}{4}F_{\mu\nu}F^{\mu\nu} + \frac{1}{2}\kappa_\psi(\partial_\psi A_\mu)(\partial^\psi A^\mu)\\ & + \frac{1}{2}\,\eta_\psi\,|\partial_\psi\Psi|^2 - \lambda_\psi\,\bar\Psi\gamma^\mu\Psi\,A_\mu^{(\psi)} - V_\psi(\Psi, A_\mu, A_\psi),\end{aligned} \tag{26}$$

where

$$D_\mu = \partial_\mu + iqA_\mu, \qquad F_{\mu\nu} = \partial_\mu A_\nu - \partial_\nu A_\mu, \tag{27}$$

and $A_\mu^{(\psi)} \equiv \partial_\psi A_\mu$ encodes the ψ-phase modulation of the gauge potential. The new terms proportional to $\kappa_\psi, \eta_\psi, \lambda_\psi$ capture dynamics along ψ; setting them to zero and $\partial_\psi(\cdot) = 0$ recovers standard QED.

Psychon Coupling (Full Equations). Psychons are excitations in the ψ-sector represented by a scalar (or spinor) field $\chi(x,\psi)$ that modulates quantum phase. A gauge-invariant coupling to QED can be written as

$$\begin{aligned}\mathcal{L}_{\text{psychon}} = {}& \frac{1}{2}(\partial_\mu\chi)(\partial^\mu\chi) + \frac{1}{2}(\partial_\psi\chi)^2 - U(\chi)\\ & - g_{\chi A}\,\chi\,F_{\mu\nu}F^{\mu\nu} - g_{\chi\tilde A}\,\chi\,F_{\mu\nu}\tilde F^{\mu\nu} - g_{\chi\psi}\,\chi\,\bar\Psi\Psi,\end{aligned} \tag{28}$$

with $\tilde F^{\mu\nu} = \frac{1}{2}\varepsilon^{\mu\nu\alpha\beta}F_{\alpha\beta}$. The Euler–Lagrange equations yield

$$\partial_\mu F^{\mu\nu} + 2g_{\chi A}\,\partial_\mu(\chi F^{\mu\nu}) + 2g_{\chi\tilde A}\,\partial_\mu(\chi\tilde F^{\mu\nu}) = q\bar\Psi\gamma^\nu\Psi + \lambda_\psi\,\partial_\psi(\bar\Psi\gamma^\nu\Psi), \tag{29}$$

$$(i\gamma^\mu D_\mu - m)\Psi - g_{\chi\psi}\,\chi\,\Psi - i\eta_\psi\,\partial_\psi^2\Psi = 0, \tag{30}$$

$$\Box\chi + \partial_\psi^2\chi + U'(\chi) = g_{\chi A}\,F_{\mu\nu}F^{\mu\nu} + g_{\chi\tilde A}\,F_{\mu\nu}\tilde F^{\mu\nu} + g_{\chi\psi}\,\bar\Psi\Psi. \tag{31}$$

These equations show how psychon dynamics can produce effective, potentially observable modulations of electromagnetic propagation and fermion masses when $\partial_\psi\chi \neq 0$.

Fokker–Planck and Phase Diffusion in ψ. The phase coordinate can exhibit stochastic dynamics governed by an effective Fokker–Planck (FP) operator acting on probability amplitude $\mathcal{P}(\psi; x)$,

$$\frac{\partial\mathcal{P}}{\partial t} = -\frac{\partial}{\partial\psi}\big[a(\psi;x)\,\mathcal{P}\big] + \frac{\partial^2}{\partial\psi^2}\big[D(\psi;x)\,\mathcal{P}\big], \tag{32}$$

inducing decoherence-like corrections to QED correlators via ψ-averaging. In the field theory, this enters as ψ-nonlocal terms or as effective η_ψ, κ_ψ renormalization.

Periodic/Quasiperiodic Solutions and Jacobi Theta Functions. If ψ is compact or effectively periodic, field modes admit expansions in Jacobi theta functions, e.g. for an EM mode amplitude A_μ:

$$A_\mu(x,\psi) = \sum_{n\in\mathbb{Z}} a_{\mu,n}(x)\,\vartheta\left[\begin{array}{c}\alpha\\ \beta\end{array}\right](n\psi\,|\,\tau_\psi), \tag{33}$$

leading to discrete sideband structures and possible fine phase quantization (see Appendix E for the α-phase analysis).

Predictions and Testable Consequences. In regimes where ∂_ψ-dynamics is small but nonzero:

- Tiny, frequency-dependent phase shifts in photon propagation (vacuum birefringence-like effects).
- Modulations of fermion effective masses $m \to m + g_{\chi\psi}\langle\chi\rangle$ in controlled resonator environments.
- Sideband structure in precision spectroscopy due to ψ-periodic components.
- No contradiction with standard QED where $\partial_\psi(\cdot) = 0$; all classic precision tests remain intact.

QED $\leftrightarrow$ UBT Mapping

QED Concept	**UBT Analogue**	**Relation/Limit**
A_μ	$\Pi_{U(1)}[\mathcal{A}_\mu(\Theta)]$	Project at constant ψ
$U(1)$	$U(1)$ extended by ψ	$\alpha = \alpha(x,\tau)$
ψ (Dirac)	Fermionic sector of Θ	Same spinor rep. at $\partial_\psi = 0$
Photon	Gauge boson in ψ-const. sector	Identical observables
Renormalization	Preserved in QED limit	ψ-terms renormalize to zero

Concluding Remarks

QED is fully recovered as the $\psi = \text{const}$ limit of the UBT electromagnetic sector. The UBT extension provides a controlled way to explore small, phase-mediated deviations without spoiling the extraordinary agreement of QED with experiment. Dedicated resonator setups and precision spectroscopy are the natural arenas to test the predicted effects.

B UBT Extension of QED

In the framework of the Unified Biquaternion Theory (UBT), Quantum Electrodynamics (QED) is naturally embedded within a richer algebraic and geometric structure. The standard space-time coordinates are extended into a *complex time* manifold

$$\tau = t + i\psi\,, \tag{34}$$

where t is the conventional temporal coordinate and ψ is the *phase-time* coordinate associated with consciousness and topological phase structure.

The electromagnetic field is promoted from the classical 4-potential A_μ to a *biquaternionic field* $\Theta(q,\tau)$, where

$$q \in \mathbb{B}\,, \quad \tau \in \mathbb{C}\,, \tag{35}$$

and $\mathbb{B}$ denotes the biquaternion algebra. This field can be expanded as

$$\Theta(q,\tau) = \sum_{\alpha=0}^{3} e_\alpha \, \Theta^\alpha(q,\tau)\,, \tag{36}$$

with e_α forming the quaternionic basis and Θ^α complex scalar functions.

The conventional QED Lagrangian

$$\mathcal{L}_{\text{QED}} = \bar{\psi}(i\gamma^\mu D_\mu - m)\psi - \frac{1}{4}F_{\mu\nu}F^{\mu\nu} \tag{37}$$

is generalized to

$$\mathcal{L}_{\text{UBT}-\text{QED}} = \bar{\Psi}\left[i\Gamma^A \nabla_A - M\right]\Psi - \frac{1}{4}\mathcal{F}_{AB}\mathcal{F}^{AB} + \mathcal{L}_{\text{psychon}} + \mathcal{L}_{\text{int}}\,, \tag{38}$$

where:

- Indices A, B run over the extended complex-time manifold,
- Γ^A are generalized gamma matrices compatible with the biquaternionic structure,
- $\mathcal{F}_{AB} = \nabla_A \mathcal{A}_B - \nabla_B \mathcal{A}_A$ is the extended field strength,
- $\mathcal{L}_{\text{psychon}}$ encodes the dynamics of *psychons* — quanta of consciousness phase,
- $\mathcal{L}_{\text{int}}$ describes couplings between electromagnetic fields and psychons.

A minimal coupling term to psychons can be written as

$$\mathcal{L}_{\text{int}} = -g_\psi \, J_A^\psi \, \mathcal{A}^A\,, \tag{39}$$

where g_ψ is the coupling constant in the phase-time direction and J_A^ψ is the psychon current.

Gauge invariance is preserved under the transformation

$$\Theta(q,\tau) \mapsto e^{i\Lambda(q,\tau)}\,\Theta(q,\tau)\,, \tag{40}$$

with $\Lambda(q,\tau)$ a biquaternion-valued gauge function. In the special case where Λ depends only on ψ, this corresponds to a pure phase-time gauge transformation, potentially observable through shifts in interference patterns or quantum phase measurements.

Interpretation. Within UBT, the Θ field is more than a gauge field — it represents the *principle of the Universe*, encapsulating both physical interactions and the phase structure of consciousness. In this light, QED appears as the $U(1)$ projection of a deeper biquaternionic gauge symmetry.

Predictions and Experimental Tests. Potential measurable effects include:

- Small deviations in electron anomalous magnetic moment a_e due to psychon coupling.
- Phase anomalies in long-baseline interferometry sensitive to ψ-dependent gauge phases.
- Modifications to vacuum birefringence in strong-field QED experiments.

C Appendix E: Standard Model Coupling and QCD Embedding in UBT

C.1 Overview

This appendix restores and consolidates the linkage between the Unified Biquaternion Theory (UBT) and the Standard Model (SM) gauge structure, with special emphasis on the QCD sector. We present a consistent dictionary from the UBT geometric variables to the SM gauge potentials and field strengths, and we state matching conditions and running-coupling relations compatible with Appendices **??** and **??**.

C.2 Gauge bundle and connections

Let the SM gauge group be

$$\mathbb{G} \;\cong\; SU(3)_c \times SU(2)_L \times U(1)_Y \,.$$

We introduce gauge connections (one-forms) and field strengths:

$$G_\mu \;=\; G_\mu^a T^a \in \mathfrak{su}(3), \qquad G_{\mu\nu} = \partial_\mu G_\nu - \partial_\nu G_\mu + i g_s \,[G_\mu, G_\nu], \tag{41}$$

$$W_\mu \;=\; W_\mu^i \tau^i \in \mathfrak{su}(2), \qquad W_{\mu\nu} = \partial_\mu W_\nu - \partial_\nu W_\mu + i g \,[W_\mu, W_\nu], \tag{42}$$

$$B_\mu \in \mathfrak{u}(1), \qquad B_{\mu\nu} = \partial_\mu B_\nu - \partial_\nu B_\mu. \tag{43}$$

The covariant derivative acting on a matter field Ψ in a representation $(\mathbf{3}, \mathbf{2}, Y)$ reads

$$D_\mu \Psi \;=\; \Big(\partial_\mu + i g_s G_\mu^a T^a + i g W_\mu^i \tau^i + i g' Y B_\mu\Big)\Psi. \tag{44}$$

C.3 UBT → SM dictionary

UBT provides a unified connection $\mathcal{A}_\mu$ on the ψ-fibered spacetime. We assume a block-diagonal projection

$$\mathcal{A}_\mu \;\longmapsto\; (G_\mu,\, W_\mu,\, B_\mu) \tag{45}$$

such that the $U(1)$ normalization is fixed by the Chern quantization as in Appendix **??**. The electric charge operator obeys $Q = T^3 + Y/2$, and the electroweak mixing is

$$\begin{pmatrix} A_\mu \\ Z_\mu \end{pmatrix} \;=\; \begin{pmatrix} \cos\theta_W & \sin\theta_W \\ -\sin\theta_W & \cos\theta_W \end{pmatrix} \begin{pmatrix} B_\mu \\ W_\mu^3 \end{pmatrix}, \qquad e \;=\; g \sin\theta_W \;=\; g' \cos\theta_W. \tag{46}$$

At low energies e matches α propose in Appendix **??**. The determination of θ_W and (g, g') requires additional matching conditions (left for future work) or a unification hypothesis.

C.4 Gauge-invariant Lagrangian

The gauge kinetic terms are

$$\mathcal{L}_{\text{gauge}} \;=\; -\frac{1}{4}\, G_{\mu\nu}^a G^{a\,\mu\nu} \;-\; \frac{1}{4}\, W_{\mu\nu}^i W^{i\,\mu\nu} \;-\; \frac{1}{4}\, B_{\mu\nu} B^{\mu\nu}. \tag{47}$$

For QCD with n_f quark flavors the matter part includes

$$\mathcal{L}_{\text{QCD}}^{\text{matter}} \;=\; \sum_{f=1}^{n_f} \bar{q}_f \,(i\gamma^\mu D_\mu - m_f)\, q_f \,, \qquad D_\mu q \;=\; (\partial_\mu + i g_s G_\mu^a T^a) q. \tag{48}$$

C.5 Running couplings and matching

QED. The low-energy fine-structure constant $\alpha(\mu)$ is fixed by the UBT topological integer N and vacuum polarization as in Appendix **??**.

QCD. The strong coupling runs according to

$$\alpha_s(\mu) \;=\; \frac{g_s^2(\mu)}{4\pi} \;=\; \frac{1}{\beta_0 \ln(\mu^2/\Lambda_{\rm QCD}^2)}\Big(1 - \frac{\beta_1}{\beta_0^2}\frac{\ln\ln(\mu^2/\Lambda_{\rm QCD}^2)}{\ln(\mu^2/\Lambda_{\rm QCD}^2)} + \cdots\Big), \tag{49}$$

with $\beta_0 = \frac{11}{4\pi} - \frac{n_f}{6\pi}$ and $\beta_1 = \frac{102}{(4\pi)^2} - \frac{38\,n_f}{(4\pi)^2}$ in the $\overline{\rm MS}$ scheme. Asymptotic freedom ($\beta_0 > 0$) and confinement at low μ are consistent with a knotted-flux interpretation in the Θ sector.

C.6 Topological interpretation of QCD in UBT

Color flux tubes correspond to knotted configurations of Θ with nontrivial linking. Wilson loops $\langle \mathrm{Tr}\,\mathcal{P}\exp i\oint G\rangle$ map to holonomies of $\mathcal{A}_\mu$ in the UBT fiber; an area law for large loops is compatible with an energy cost proportional to knotted tube length and curvature. Instanton sectors ($\pi_3(SU(2)) \cong \mathbb{Z}$) mirror Hopf-like textures, providing a common topological language for both EM and QCD sectors.

C.7 Matching conditions and open tasks

- **Normalization:** $U(1)$ is fixed by Chern quantization (Appendix **??**). The QCD normalization is anchored by $\Lambda_{\rm QCD}$; in UBT one expects $\Lambda_{\rm QCD} \sim \xi\,\mu_{\rm int}$, with the internal-mode scale $\mu_{\rm int}$ from the electron sector and $\xi = \mathcal{O}(1)$ to be fitted.
- **Electroweak mixing:** determining θ_W from UBT requires an additional symmetry or a unification hypothesis; otherwise it is an independent parameter.
- **Anomalies:** the SM matter assignment must satisfy anomaly cancellation; UBT embeddings should preserve this (check fermion content mapping).
- **Hadron phenomenology:** flux-tube/knotted-state spectra vs. lattice-QCD input is an avenue for quantitative tests.

C.8 Consistency with dark matter appendix

The interaction portals between the Θ topological sector and colored matter are suppressed by orthogonality (complex-time fiber) and higher-dimensional operators. Therefore QCD does not spoil the DM stability discussed in Appendix **??**, while gravitational coupling remains universal.

Appendix K: Maxwell Fields in Curved Spacetime (Bessel and Hankel Solutions)

K.1 UBT Motivation and Setting

In the Unified Biquaternion Theory (UBT), the master field $\Theta(q,\tau)$ lives on a complexified spacetime with $\tau = t + i\psi$. Electromagnetic (EM) excitations are described by a $U(1)$ sector coupled to Θ, and their propagation in curved geometry is central for laboratory protocols (Appendix E) and for metric back-reaction studies (Appendix J). Here we develop Maxwell theory on a curved background, recovering *Bessel* and *Hankel* structures for axisymmetric configurations and summarizing boundary conditions relevant to UBT experiments.

K.2 Maxwell Equations on a Curved Background

Using metric signature $(-,+,+,+)$, the vacuum Maxwell equations read

$$\nabla_\nu F^{\mu\nu} = \mu_0 J^\mu, \qquad \nabla_{[\alpha} F_{\beta\gamma]} = 0, \tag{50}$$

with $F_{\mu\nu} = \partial_\mu A_\nu - \partial_\nu A_\mu$, ∇ the Levi–Civita covariant derivative of $g_{\mu\nu}$. In index-expanded form,

$$\frac{1}{\sqrt{-g}} \partial_\nu \big(\sqrt{-g}\, F^{\mu\nu}\big) = \mu_0 J^\mu. \tag{51}$$

For stationary, axisymmetric backgrounds (e.g. a weakly rotating metric or a cylindrical chart) and harmonic time dependence $e^{-i\omega t}$, the field equations reduce to scalar Helmholtz-type equations for the longitudinal potentials/components, with a geometry-dependent effective index.

K.3 Cylindrical Separation and Bessel/Hankel Structure

In cylindrical coordinates (ρ, ϕ, z) with axial symmetry and $\partial_z = 0$, a representative scalar mode $U(\rho,\phi,t) = R(\rho)\, e^{im\phi} e^{-i\omega t}$ obeys

$$\frac{1}{\rho}\frac{d}{d\rho}\left(\rho \frac{dR}{d\rho}\right) - \frac{m^2}{\rho^2} R + k_\perp^2 R = 0, \qquad k_\perp^2 = n_{\text{eff}}^2(\omega, \text{metric})\, \frac{\omega^2}{c^2}, \tag{52}$$

with solutions

$$R(\rho) = A\, J_m(k_\perp \rho) + B\, Y_m(k_\perp \rho), \qquad \text{outgoing waves: } R(\rho) \propto H_m^{(1)}(k_\perp \rho). \tag{53}$$

Here J_m and Y_m are Bessel functions of first and second kind; $H_m^{(1)} = J_m + iY_m$ is the outgoing Hankel function. Curvature and frame-dragging enter n_{eff} and cross-couplings among polarizations (Appendix J).

K.4 Boundary Conditions (PEC Cylinder, TE/TM Selection)

For a perfect electric conductor (PEC) of radius a, the standard boundary conditions yield discrete transverse wavenumbers $k_{\perp,mn}$. For TM_{mn} (axial E_z nonzero): $J_m(k_{\perp,mn} a) = 0$; for TE_{mn} (axial H_z nonzero): $J_m'(k_{\perp,mn} a) = 0$. The lowest zeros are $x_{0,1} \approx 2.4048$ for J_0 and $x_{0,1}' = x_{1,1} \approx 3.8317$ for J_0' (i.e. the first zero of J_1).

K.5 ISM-Band Examples (Radius Estimates)

For frequency f (wavenumber $k = 2\pi f/c$), a cylindrical cavity supporting TM_{01} or TE_{01} has approximate radii $a \approx x_{0,1}/k$ and $a \approx x_{0,1}'/k$, respectively. Table 1 gives indicative values for common ISM bands assuming vacuum ($n_{\text{eff}} = 1$). Curved backgrounds shift these via $n_{\text{eff}}(\omega)$.

f [GHz]	k [m^{-1}]	a_{TM01} [mm]	a_{TE01} [mm]
2.40	50.30	47.81	76.18
5.00	104.79	22.95	36.56
10.00	209.58	11.47	18.28

Table 1: Indicative cavity radii for TM_{01} (J_0 zero) and TE_{01} (J_0' zero) at ISM-like frequencies.

K.6 Plots (Embedded Data; No External Figures)

Figures 1 and 2 include inline data generated from Bessel and Hankel functions.

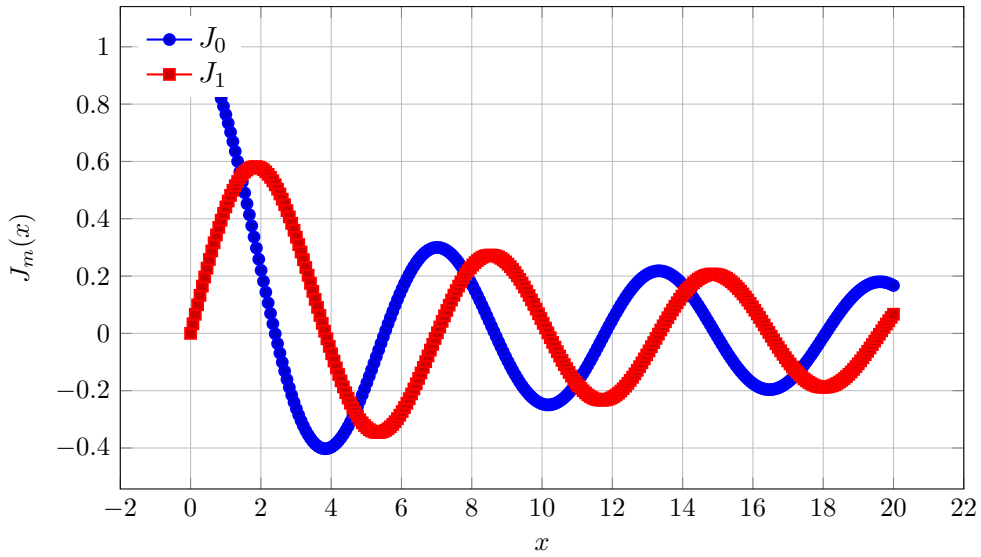

Figure 1: Bessel functions J_0 and J_1 relevant for TM/TE mode selection in cylindrical symmetry.

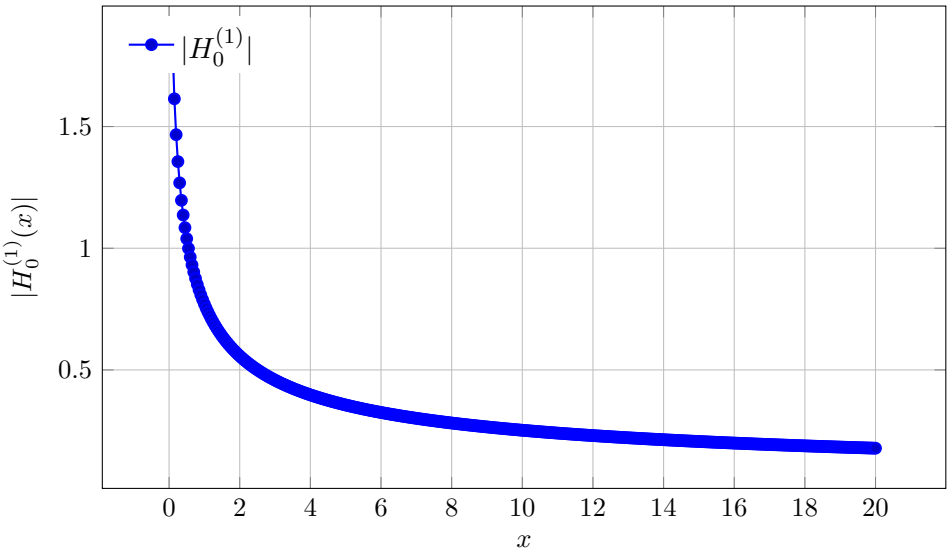

Figure 2: Magnitude of the outgoing Hankel function $H_0^{(1)} = J_0 + iY_0$.

K.7 Curved-Space Corrections and UBT Links

Weak curvature and frame-dragging modify the separation constant via an effective index $n_{\text{eff}}(\omega, \text{metric})$ and couple polarizations in the transport equations (eikonal limit). Within UBT, slow ψ-sector deformations shift dispersion and boundary spectra ($k_{\perp,mn} \to k_{\perp,mn} + \delta k_\perp(\psi)$), yielding measurable changes in cavity frequencies and scattering phase (cross-reference: Appendix I, J, E). These provide direct targets for metrology and for bounding the ψ-sector couplings.

K.8 Summary

Maxwell fields on curved backgrounds separate to Bessel/Hankel radial profiles under axial symmetry. PEC boundaries quantize $k_\perp$ via zeros of J_m or J'_m; curved-space and UBT ψ-sector effects enter as shifts of the effective index and mode spectrum. The ISM-band radius estimates connect theory to buildable experiments, while embedded plots serve as quick references for

J_0, J_1, and $|H_0^{(1)}|$.

A Appendix P: Bibliography

References

B Policy on the Fine-Structure Constant

In the CORE manuscript we do not claim an ab-initio derivation of α. We adopt $\alpha(\mu)$ with standard QED running and treat $\alpha(\mu_0)$ as an empirical input. Discrete prime/p-adic or entropic models are exploratory and documented separately in the Speculative Notes.